

SEAFORMER: SQUEEZE-ENHANCED AXIAL TRANSFORMER FOR MOBILE SEMANTIC SEGMENTATION

Qiang Wan^{1*}, Zilong Huang², Jiachen Lu¹, Gang Yu², Li Zhang^{1†}

¹School of Data Science, Fudan University ²Tencent PCG

ABSTRACT

Since the introduction of Vision Transformers, the landscape of many computer vision tasks (*e.g.*, semantic segmentation), which has been overwhelmingly dominated by CNNs, recently has significantly revolutionized. However, the computational cost and memory requirement render these methods unsuitable on the mobile device, especially for the high-resolution per-pixel semantic segmentation task. In this paper, we introduce a new method *squeeze-enhanced Axial Transformer (SeaFormer)* for mobile semantic segmentation. Specifically, we design a generic attention block characterized by the formulation of squeeze Axial and detail enhancement. It can be further used to create a family of backbone architectures with superior cost-effectiveness. Coupled with a light segmentation head, we achieve the best trade-off between segmentation accuracy and latency on the ARM-based mobile devices on the ADE20K and Cityscapes datasets. Critically, we beat both the mobile-friendly rivals and Transformer-based counterparts with better performance and lower latency without bells and whistles. Beyond semantic segmentation, we further apply the proposed SeaFormer architecture to image classification problem, demonstrating the potentials of serving as a versatile mobile-friendly backbone. Our code and models are made publicly available at <https://github.com/fudan-zvg/SeaFormer>.

1 INTRODUCTION

As a fundamental problem in computer vision, semantic segmentation aims to assign a semantic class label to each pixel in an image. Conventional methods rely on stacking local convolution kernel Long et al. (2015) to perceive the long-range structure information of the image.

Since the introduction of Vision Transformers Dosovitskiy et al. (2021), the landscape of semantic segmentation has significantly revolutionized. Transformer-based approaches Zheng et al. (2021); Xie et al. (2021) have remarkably demonstrated the capability of global context modeling. However, the computational cost and memory requirement of Transformer render these methods unsuitable on mobile devices, especially for high-resolution imagery inputs.

Following conventional wisdom of efficient operation, local/window-based attention Luong et al. (2015); Liu et al. (2021); Huang et al. (2021a); Yuan et al. (2021), Axial attention Huang et al. (2019b); Ho et al. (2019); Wang et al. (2020a), dynamic graph message passing Zhang et al. (2020; 2022b) and some lightweight attention mechanisms Hou et al. (2020); Li et al. (2021b;c; 2020); Liu et al. (2018); Shen et al. (2021); Xu et al. (2021); Cao et al. (2019); Woo et al. (2018); Wang et al. (2020b); Choromanski et al. (2021); Chen et al. (2017); Mehta & Rastegari (2022a) are introduced.

However, these advances are still insufficient to satisfy the design requirements and constraints for mobile devices due to the high latency on the high-resolution inputs (see Figure 1). Recently there is a surge of interest in building a Transformer-based semantic segmentation. In order to reduce the computation cost at high resolution, TopFormer Zhang et al. (2022c) dedicates to applying the global attention at a $1/64$ scale of the original input, which definitely harms the segmentation performance.

To solve the dilemma of high-resolution computation for pixel-wise segmentation task and low latency requirement on the mobile device in a performance harmless way, we propose a family

*Work done while Qiang Wan was an intern at Tencent GY-Lab.

†Corresponding author: lizhangfd@fudan.edu.cn

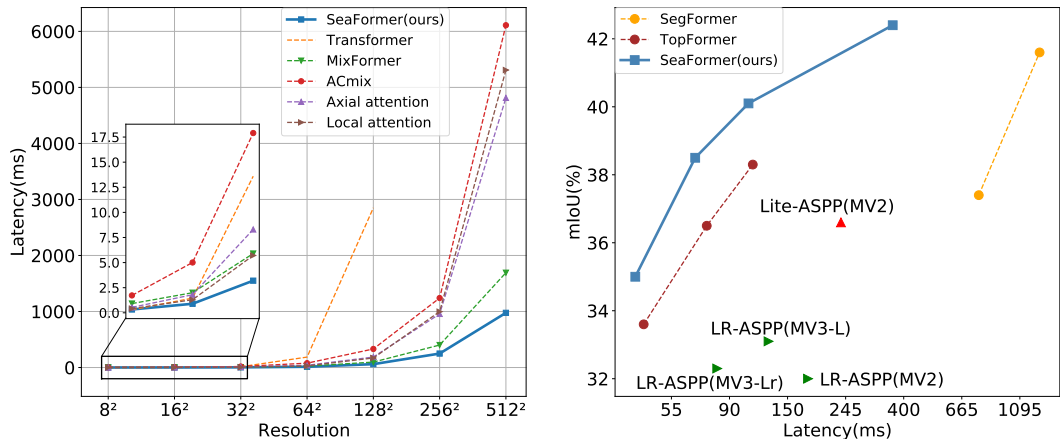


Figure 1: **Left:** Latency comparison with Transformer Vaswani et al. (2017), MixFormer Chen et al. (2022a), ACmix Pan et al. (2022b), Axial attention Ho et al. (2019) and local attention Luong et al. (2015). It is measured with a single module of channel dimension 64 on a Qualcomm Snapdragon 865 processor. **Right:** The mIoU versus latency on the ADE20K *val* set. MV2 means MobileNetV2 Sandler et al. (2018). MV3-L means MobileNetV3-Large Howard et al. (2019). MV3-Lr denotes MobileNetV3-Large-reduce Howard et al. (2019). The latency is measured on a single Qualcomm Snapdragon 865, and only an ARM CPU core is used for speed testing. No other means of acceleration, e.g., GPU or quantification, is used. For figure *Right*, the input size is 512×512. SeaFormer achieves superior trade-off between mIoU and latency.

of mobile-friendly Transformer-based semantic segmentation model, dubbed as *squeeze-enhanced Axial Transformer* (SeaFormer), which reduces the computational complexity of axial attention from $\mathcal{O}((H+W)HW)$ to $\mathcal{O}(HW)$, to achieve superior accuracy-efficiency trade-off on mobile devices and fill the vacancy of mobile-friendly efficient Transformer.

The core building block *squeeze-enhanced Axial attention* (SEA attention) seeks to squeeze (pool) the input feature maps along the horizontal/vertical axis into a compact column/row and computes self-attention. We concatenate query, keys and values to compensate the detail information sacrificed during squeeze and then feed it into a depth-wise convolution layer to enhance local details.

Coupled with a light segmentation head, our design (see Figure 2) with the proposed SeaFormer layer in the small-scale feature is capable of conducting high-resolution image semantic segmentation with low latency on the mobile device. As shown in Figure 1, the proposed SeaFormer outperforms other efficient neural networks on the ADE20K dataset with lower latency. In particular, SeaFormer-Base is superior to the lightweight CNN counterpart MobileNetV3 (41.0 vs.33.1 mIoU) with lower latency (106ms vs.126ms) on an ARM-based mobile device.

We make the following **contributions**: **(i)** We introduce a novel *squeeze-enhanced Axial Transformer* (SeaFormer) framework for mobile semantic segmentation; **(ii)** Critically, we design a generic attention block characterized by the formulation of squeeze Axial and detail enhancement; It can be used to create a family of backbone architectures with superior cost-effectiveness; **(iii)** We show top performance on the ADE20K and Cityscapes datasets, beating both the mobile-friendly rival and Transformer-based segmentation model with clear margins; **(iv)** Beyond semantic segmentation, we further apply the proposed SeaFormer architecture to the image classification problem, demonstrating the potential of serving as a versatile mobile-friendly backbone.

2 RELATED WORK

Combination of Transformers and convolution Convolution is relatively efficient but not suitable to capture long-range dependencies and vision Transformer has the powerful capability with a global receptive field but lacks efficiency due to the computation of self-attention. In order to make full use of both of their advantages, MobileViT Mehta & Rastegari (2022a), TopFormer Zhang et al. (2022c), LVT Yang et al. (2022), MobileFormer Chen et al. (2022b), EdgeViTs Pan et al. (2022a), MobileViTv2 Mehta & Rastegari (2022b), EdgeFormer Zhang et al. (2022a) and EfficientFormer Li et al. (2022) are constructed as efficient ViTs by combining convolution with Transformers. Mobile-

ViT, Mobile-Former, TopFormer and EfficientFormer are restricted by Transformer blocks and have to trade off between efficiency and performance in model design. LVT, MobileViTv2 and EdgeViTs keep the model size small at the cost of relatively high computation, which also means high latency.

Axial attention and variants Axial attention Huang et al. (2019b); Ho et al. (2019); Wang et al. (2020a) is designed to reduce the computational complexity of original global self-attention Vaswani et al. (2017). It computes self-attention over a single axis at a time and stacks a horizontal and a vertical axial attention module to obtain the global receptive field. Strip pooling Hou et al. (2020) and Coordinate attention Hou et al. (2021) uses a band shape pooling window to pool along either the horizontal or the vertical dimension to gather long-range context. Kronecker Attention Networks Gao et al. (2020) uses the juxtaposition of horizontal and lateral average matrices to average the input matrices and performs attention operation. These methods and other similar implementations provide performance gains partly at considerably low computational cost compared with Axial attention. However, they ignore the lack of local details brought by the pooling/average operation.

Mobile semantic segmentation The mainstream of efficient segmentation methods are based on lightweight CNNs. DFANet Li et al. (2019) adopts a lightweight backbone to reduce computation cost and adds a feature aggregation module to refine high-level and low-level features. ICNet Zhao et al. (2018) designs an image cascade network to speed up the algorithm, while BiSeNet Yu et al. (2018; 2021) proposes two-stream paths for low-level details and high-level context information, separately. Fast-SCNN Poudel et al. (2019) shares the computational cost of the multi-branch network to yield a run-time fast segmentation CNN. TopFormer Zhang et al. (2022c) presents a new architecture with a combination of CNNs and ViT and achieves a good trade-off between accuracy and computational cost for mobile semantic segmentation. However, it is still restricted by the heavy computation load of global self-attention.

3 METHOD

3.1 OVERALL ARCHITECTURE

Inspired by the two-branch architectures Yu et al. (2021); Poudel et al. (2019); Hong et al. (2021); Huang et al. (2021b); Chen et al. (2022b), we design a **squeeze-enhanced Axial Transformer (SeaFormer)** framework. As is shown in Figure 2, SeaFormer consists of these parts: *shared STEM*, *context branch*, *spatial branch*, *fusion block* and *light segmentation head*. For a fair comparison, we follow TopFormer Zhang et al. (2022c) to design the STEM. It consists of one regular convolution with stride of 2 followed by four MobileNet blocks where stride of the first and third block is 2. The context branch and the spatial branch share the produced feature map, which allows us to build a fast semantic segmentation model.

Context branch The context branch is designed to capture context-rich information from the feature map x_s . As illustrated in the red branch of Figure 2, the context branch is divided into three stages. To obtain larger receptive field, we stack SeaFormer layers after applying a MobileNet block to down-sampling and expanding feature dimension. Compared with the standard convolution as the down-sampling module, MobileNet block increases the representation capacity of the model while maintaining a lower amount of computation and latency. For variants except SeaFormer-Large, SeaFormer layers are applied in the last two stages for superior trade-off between accuracy and efficiency. For SeaFormer-Large, we insert SeaFormer layers in each stage of context branch. To achieve a good trade-off between segmentation accuracy and inference speed, we design a squeeze-enhanced Axial attention block (SEA attention) illustrated in the next subsection.

Spatial branch The spatial branch is designed to obtain spatial information in high resolution. Identical to the context branch, the spatial branch reuses feature maps x_s . However, the feature from the early convolution layers contains rich spatial details but lacks high-level semantic information. Consequently, we design a fusion block to fuse the features in the context branch into the spatial branch, bringing high-level semantic information into the low-level spatial information.

Fusion block As depicted in Figure 2, high resolution feature maps in the spatial branch are followed by a 1×1 convolution and a batch normalization layer to produce a feature to fuse. Low

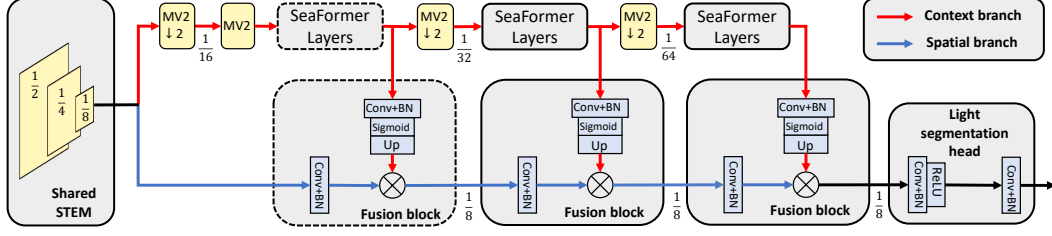


Figure 2: The overall architecture of SeaFormer. It contains shared STEM, context branch (red), spatial branch (blue), fusion block and light segmentation head. MV2 block means MobileNetV2 block and MV2 ↓2 means MobileNetV2 block with downsampling. SeaFormer layers and fusion block with dash box only exist in SeaFormer-L. The symbol \otimes denotes element-wise multiplication.

resolution feature maps in the context branch are fed into a 1×1 convolution layer, a batch normalization layer, a sigmoid layer and up-sampled to high resolution to produce semantics weights by bilinear interpolation. Then, the semantics weights from context branch are element-wisely multiplied to the high resolution feature from spatial branch. The fusion block enables low-level spatial features to obtain high-level semantic information.

Light segmentation head The feature after the last fusion block is fed into the proposed segmentation head directly, as demonstrated in Figure 2. For fast inference purpose, our light segmentation head consists of two convolution layers, which are followed by a batch normalization layer separately and the feature from the first batch normalization layer is fed into an activation layer.

3.2 SQUEEZE-ENHANCED AXIAL ATTENTION

The global attention can be expressed as

$$\mathbf{y}_o = \sum_{p \in \mathcal{G}(o)} \text{softmax}_p(\mathbf{q}_o^\top \mathbf{k}_p) \mathbf{v}_p \quad (1)$$

where $\mathbf{x} \in \mathbb{R}^{H \times W \times C}$. $\mathbf{q}, \mathbf{k}, \mathbf{v}$ are linear projection of \mathbf{x} , *i.e.* $\mathbf{q} = \mathbf{W}_q \mathbf{x}, \mathbf{k} = \mathbf{W}_k \mathbf{x}, \mathbf{v} = \mathbf{W}_v \mathbf{x}$, where $\mathbf{W}_q, \mathbf{W}_k \in \mathbb{R}^{C_{qk} \times C}$, $\mathbf{W}_v \in \mathbb{R}^{C_v \times C}$ are learnable weights. $\mathcal{G}(o)$ means all positions on the feature map of location $o = (i, j)$. When traditional attention module is applied on a feature map of $H \times W \times C$, the time complexity can be $\mathcal{O}(H^2 W^2 (C_{qk} + C_v))$, leading to low efficiency and high latency.

$$\mathbf{y}_o = \sum_{p \in \mathcal{N}_{m \times m}(o)} \text{softmax}_p(\mathbf{q}_o^\top \mathbf{k}_p) \mathbf{v}_p \quad (2)$$

$$\mathbf{y}_o = \sum_{p \in \mathcal{N}_{1 \times W}(o)} \text{softmax}_p(\mathbf{q}_o^\top \mathbf{k}_p) \mathbf{v}_p + \sum_{p \in \mathcal{N}_{H \times 1}(o)} \text{softmax}_p(\mathbf{q}_o^\top \mathbf{k}_p) \mathbf{v}_p \quad (3)$$

To improve the efficiency, there are some works Liu et al. (2021); Huang et al. (2019b); Ho et al. (2019) computing self-attention within the local region. We show two most representative efficient Transformer in Equation 2, 3. Equation 2 is represented by window-based attention Luong et al. (2015) successfully reducing the time complexity to $\mathcal{O}(m^2 H W (C_{qk} + C_v)) = \mathcal{O}(H W)$, where $\mathcal{N}_{m \times m}(o)$ means the neighbour $m \times m$ positions of o , but losing global receptiveness. The Equation 3 is represented by Axial attention Ho et al. (2019), which only reduces the time complexity to $\mathcal{O}((H + W) H W (C_{qk} + C_v)) = \mathcal{O}((H W)^{1.5})$, where $\mathcal{N}_{H \times 1}(o)$ means all the positions of the column of o ; $\mathcal{N}_{1 \times W}(o)$ means all the positions of the row of o .

According to their drawbacks, we propose the mobile-friendly squeeze-enhanced Axial attention, with a succinct squeeze Axial attention for global semantics extraction and an efficient convolution-based detail enhancement kernel for local details supplement.

$$\mathbf{q}_{(h)} = \frac{1}{W} \left(\mathbf{q}^{\rightarrow(C_{qk}, H, W)} \mathbf{1}_W \right)^{\rightarrow(H, C_{qk})}, \quad \mathbf{q}_{(v)} = \frac{1}{H} \left(\mathbf{q}^{\rightarrow(C_{qk}, W, H)} \mathbf{1}_H \right)^{\rightarrow(W, C_{qk})} \quad (4)$$

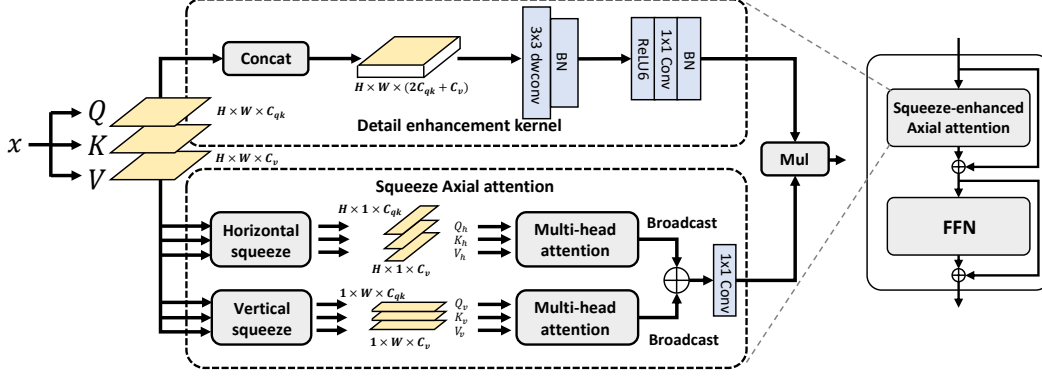


Figure 3: **Right**: the schematic illustration of the proposed squeeze-enhanced Axial Transformer layer including a squeeze-enhanced Axial attention and a Feed-Forward Network (FFN). **Left** is the squeeze-enhanced Axial Transformer layer, including detail enhancement kernel and squeeze Axial attention. The symbol \oplus indicates an element-wise addition operation. Mul means multiplication.

Squeeze Axial attention To achieve a more efficient computation and aggregate global information at the same time, we resort to a more radical strategy. In the same way, $\mathbf{q}, \mathbf{k}, \mathbf{v}$ are first get from \mathbf{x} with $\mathbf{W}_q^{(s)}, \mathbf{W}_k^{(s)} \in \mathbb{R}^{C_{qk} \times C}, \mathbf{W}_v^{(s)} \in \mathbb{R}^{C_v \times C}$. According to Equation 4, we first implement *horizontal squeeze* by taking average of query feature map on the horizontal direction. In the same way, the right shows the *vertical squeeze* on the vertical direction. $\mathbf{z}^{\rightarrow(\cdot)}$ means permuting the dimension of tensor \mathbf{z} as given, and $\mathbb{1}_m \in \mathbb{R}^m$ is a vector with all the elements equal to 1. The squeeze operation on \mathbf{q} also repeats on \mathbf{k} and \mathbf{v} , so we finally get $\mathbf{q}_{(h)}, \mathbf{k}_{(h)}, \mathbf{v}_{(h)} \in \mathbb{R}^{H \times C_{qk}}, \mathbf{q}_{(v)}, \mathbf{k}_{(v)}, \mathbf{v}_{(v)} \in \mathbb{R}^{W \times C_{qk}}$. The squeeze operation reserves the global information to a single axis, thus greatly alleviating the following global semantic extraction showing by Equation 5.

$$\mathbf{y}_{(i,j)} = \sum_{p=1}^H \text{softmax}_p \left(\mathbf{q}_{(h)i}^\top \mathbf{k}_{(h)p} \right) \mathbf{v}_{(h)p} + \sum_{p=1}^W \text{softmax}_p \left(\mathbf{q}_{(v)j}^\top \mathbf{k}_{(v)p} \right) \mathbf{v}_{(v)p} \quad (5)$$

Each position of feature map propagates information only on two squeezed axial features. Although it shows no distinct computation reduction comparing to Equation 3, repeat of Equation 5 can be simply implemented by the most efficient broadcast operation. The detail is shown in Figure 3. Time complexity for squeezing $\mathbf{q}, \mathbf{k}, \mathbf{v}$ is $\mathcal{O}((H+W)(2C_{qk} + C_v))$ and the attention operation takes $\mathcal{O}((H^2 + W^2)(C_{qk} + C_v))$ time. Thus, our squeeze Axial attention successfully reduces time complexity to $\mathcal{O}(HW)$.

Squeeze Axial position embedding Equation 4 are, however, not positional-aware, including no positional information of feature map. Hence, we propose squeeze Axial position embedding to squeeze Axial attention. For squeeze Axial attention, we render both $\mathbf{q}_{(h)}$ and $\mathbf{k}_{(h)}$ to be aware of their position in squeezed axial feature by introducing positional embedding $\mathbf{r}_{(h)}^q, \mathbf{r}_{(h)}^k \in \mathbb{R}^{H \times C_{qk}}$, which are linearly interpolated from learnable parameters $\mathbf{B}_{(h)}^q, \mathbf{B}_{(h)}^k \in \mathbb{R}^{L \times C_{qk}}$. L is a constant. In the same way, $\mathbf{r}_{(v)}^q, \mathbf{r}_{(v)}^k \in \mathbb{R}^{W \times C_{qk}}$ are applied to $\mathbf{q}_{(v)}, \mathbf{k}_{(v)}$. Thus, the positional-aware squeeze Axial attention can be expressed as Equation 6.

$$\begin{aligned} \mathbf{y}_{(i,j)} = & \sum_{p=1}^H \text{softmax}_p \left((\mathbf{q}_{(h)i} + \mathbf{r}_{(h)i}^q)^\top (\mathbf{k}_{(h)p} + \mathbf{r}_{(h)p}^k) \right) \mathbf{v}_{(h)p} \\ & + \sum_{p=1}^W \text{softmax}_p \left((\mathbf{q}_{(v)j} + \mathbf{r}_{(v)j}^q)^\top (\mathbf{k}_{(v)p} + \mathbf{r}_{(v)p}^k) \right) \mathbf{v}_{(v)p} \end{aligned} \quad (6)$$

Detail enhancement kernel The squeeze operation, though extracting global semantic information efficiently, sacrifices the local details. Hence an auxiliary convolution-based kernel is applied to enhance the spatial details. As is shown in the upper path of Figure 3, $\mathbf{q}, \mathbf{k}, \mathbf{v}$ are first get from \mathbf{x} with another $\mathbf{W}_q^{(e)}, \mathbf{W}_k^{(e)} \in \mathbb{R}^{C_{qk} \times C}, \mathbf{W}_v^{(e)} \in \mathbb{R}^{C_v \times C}$ and are concatenated on the channel dimension and then passed to a block made up of 3×3 depth-wise convolution and batch normalization.

Backbone	Decoder	Params	FLOPs	mIoU	Latency
MobileNetV2	LR-ASPP	2.2M	2.8G	32.0	177ms
MobileNetV3-Large-reduce	LR-ASPP	1.6M	1.3G	32.3	81ms
MobileNetV3-Large	LR-ASPP	3.2M	2.0G	33.1	126ms
HRNet-W18-Small	HRNet-W18-Small	4.0M	10.2G	33.4	639ms
TopFormer-T	Simple Head	1.4M	0.6G	33.6	43ms
TopFormer-T*	Simple Head	1.4M	0.6G	34.6	43ms
SeaFormer-T	Light Head	1.7M	0.6G	35.0	40ms
SeaFormer-T*	Light Head	1.7M	0.6G	35.8±0.35	40ms
ConvMLP-S	Semantic FPN	12.8M	33.8G	35.8	777ms
EfficientNet	DeepLabV3+	17.1M	26.9G	36.2	970ms
MobileNetV2	Lite-ASPP	2.9M	4.4G	36.6	235ms
TopFormer-S	Simple Head	3.1M	1.2G	36.5	74ms
TopFormer-S*	Simple Head	3.1M	1.2G	37.0	74ms
SeaFormer-S	Light Head	4.0M	1.1G	38.1	67ms
SeaFormer-S*	Light Head	4.0M	1.1G	39.4±0.25	67ms
MiT-B0	SegFormer	3.8M	8.4G	37.4	770ms
ResNet18	Lite-ASPP	12.5M	19.2G	37.5	648ms
ShuffleNetV2-1.5x	DeepLabV3+	16.9M	15.3G	37.6	960ms
MobileNetV2	DeepLabV3+	15.4M	25.8G	38.1	1035ms
TopFormer-B	Simple Head	5.1M	1.8G	38.3	110ms
TopFormer-B*	Simple Head	5.1M	1.8G	39.2	110ms
SeaFormer-B	Light Head	8.6M	1.8G	40.2	106ms
SeaFormer-B*	Light Head	8.6M	1.8G	41.0±0.45	106ms
MiT-B1	SegFormer	13.7M	15.9G	41.6	1300ms
SeaFormer-L	Light Head	14.0M	6.5G	42.7	367ms
SeaFormer-L*	Light Head	14.0M	6.5G	43.7±0.36	367ms

Table 1: Results of semantic segmentation on ADE20K *val* set, * indicates training batch size is 32. The latency is measured on a single Qualcomm Snapdragon 865 with input size 512×512, and only an ARM CPU core is used for speed testing. References: MobileNetV2 Sandler et al. (2018), MobileNetV3 Howard et al. (2019), HRNet Yuan et al. (2020), TopFormer Zhang et al. (2022c), ConvMLP Li et al. (2021a), Semantic FPN Kirillov et al. (2019), EfficientNet Tan & Le (2019), DeepLabV3+ and Lite-ASPP Chen et al. (2018a), SegFormer Xie et al. (2021), ResNet He et al. (2016), ShuffleNetV2-1.5x Ma et al. (2018).

By using a 3×3 convolution, auxiliary local details can be aggregated from $\mathbf{q}, \mathbf{k}, \mathbf{v}$. And then a linear projection with activation function and batch normalization are used to squeeze ($2C_{qk} + C_v$) dimension to C and generate detail enhancement weights. Finally, the enhancement feature will be fused with the feature given by squeeze Axial attention. Different enhancement mode including element-wise addition and multiplication will be compared in experiment section. Time complexity for the 3×3 depth-wise convolution is $\mathcal{O}(3^2HW(2C_{qk} + C_v))$ and the time complexity for the 1×1 convolution is $\mathcal{O}(HWC(2C_{qk} + C_v))$. Time for the other operations like activation can be omitted.

Architecture and Variants We introduce four variants, SeaFormer-Tiny, Small, Base and Large (T, S, B and L). More configuration details are listed in the supplementary material.

4 EXPERIMENTS

We evaluate our method on semantic segmentation and image classification tasks. First, we describe implementation details and compare results with state of the art. We then conduct a series of ablation studies to validate the design of SeaFormer. Each proposed component and important hyper-parameters are examined thoroughly.

4.1 EXPERIMENTAL SETUP

4.1.1 DATASET

We perform segmentation experiments over ADE20K Zhou et al. (2017), CityScapes Cordts et al. (2016). The mean of intersection over union (mIoU) is set as the evaluation metric. We convert full-precision models to TNN Contributors (2019) and measure latency on an ARM-based device with a single Qualcomm Snapdragon 865 processor.

Method	Backbone	FLOPs	mIoU(val)	mIoU(test)	Latency
FCN	MobileNetV2	317G	61.5	-	24190ms
PSPNet	MobileNetV2	423G	70.2	-	31440ms
SegFormer(h)	MiT-B0	17.7G	71.9	-	1586ms
SegFormer(f)	MiT-B0	125.5G	76.2	-	11030ms
L-ASPP	MobileNetV2	12.6G	72.7	-	887ms
LR-ASPP	MobileNetV3-L	9.7G	72.4	72.6	660ms
LR-ASPP	MobileNetV3-S	2.9G	68.4	69.4	211ms
Simple Head(h)	TopFormer-B	2.7G	70.7	-	173ms
Simple Head(f)	TopFormer-B	11.2G	75.0	75.0	749ms
Light Head(h)	SeaFormer-S	2.0G	70.7	71.0	129ms
Light Head(f)	SeaFormer-S	8.0G	76.1	75.9	518ms
Light Head(h)	SeaFormer-B	3.4G	72.2	72.5	205ms
Light Head(f)	SeaFormer-B	13.7G	77.7	77.5	821ms

Table 2: Results on Cityscapes *val* set. The results on *test* set of some methods are not presented due to the fact that they are not reported in their original papers.

ADE20K dataset covers 150 categories, containing 25K images that are split into 20K/2K/3K for *Train*, *val* and *test*. **CityScapes** is a driving dataset for semantic segmentation. It consists of 5000 fine annotated high-resolution images with 19 categories.

4.1.2 IMPLEMENTATION DETAILS

We set ImageNet-1K Deng et al. (2009) pretrained network as the backbone, and training details of ImageNet-1K are illustrated in the last subsection. For semantic segmentation, the standard Batch-Norm Ioffe & Szegedy (2015) layer is replaced by synchronized BatchNorm.

Training Our implementation is based on public codebase `mmsegmentation` Contributors (2020). We follow the batch size, training iteration scheduler and data augmentation strategy of TopFormer Zhang et al. (2022c) for a fair comparison. The initial learning rate is 0.0005 and the weight decay is 0.01. A “poly” learning rate scheduled with factor 1.0 is adopted. During inference, we set the same resize and crop rules as TopFormer to ensure fairness. The comparison of Cityscapes contains full-resolution and half-resolution. For the full-resolution version, the training images are randomly scaled and then cropped to the fixed size of 1024×1024 . For the half-resolution version, the training images are resized to 1024×512 and randomly scaling, the crop size is 1024×512 .

4.2 COMPARISON WITH STATE OF THE ART

ADE20K Table 1 shows the results of SeaFormer and previous efficient backbones on ADE20K *val* set. The comparison covers Params, FLOPs, Latency and mIoU. As shown in Table 1, SeaFormer outperforms these approaches with comparable or less FLOPs and lower latency. Compared with specially designed mobile backbone, TopFormer, which sets global attention as its semantics extractor, SeaFormer achieves higher segmentation accuracy with lower latency. And the performance of SeaFormer-B surpasses MobileNetV3 by a large margin of +7.9% mIoU with lower latency (-16%). The results demonstrate our SeaFormer layers improve the representation capability significantly.

Cityscapes From the table 2, it can be seen that SeaFormer-S achieves comparable or better results than TopFormer-B with less computation cost and latency, which proves that SeaFormer could also achieve a good trade-off between performance and latency in high-resolution scenario.

4.3 ABLATION STUDIES

In this section, we ablate different self-attention implementations and some important design elements in the proposed model, including our squeeze-enhanced Axial attention module (SEA attention) and fusion block on ADE20K dataset.

The influence of components in SEA attention We conduct experiments with several configurations, including detail enhancement kernel only, squeeze Axial attention only, and the fusion of both. As is shown in Table 3, only detail enhancement or squeeze Axial attention achieves a relatively poor

Enhance Attn kernel	Enhance Attn branch	Enhance input	Enhance mode	Params	FLOPs	Latency	Top1	mIoU
✓		-	-	1.3M	0.58G	38ms	65.9	32.5
	✓	-	-	1.4M	0.57G	38ms	66.3	33.5
✓	✓	conv(x)	Mul	1.6M	0.60G	40ms	67.2	34.9
✓	✓	upconv(x)	Mul	1.8M	0.62G	41ms	68.1	35.9
✓	✓	concat[qkv]	Mul	1.7M	0.60G	40ms	67.9	35.8
✓	✓	concat[qkv]	Add	1.7M	0.60G	40ms	67.3	35.4

Table 3: Ablation studies on components in SEA attention on ImageNet-1K and ADE20K datasets. Enhancement input means the input of detail enhancement kernel. conv(x) means x followed by a point-wise conv. upconv(x) is the same as conv(x) except different channels as upconv(x) is from C_{in}^i to $C_q + C_k + C_v$ and conv(x) is from C_{in} to C_{in} . concat[qkv] indicates concat of Q,K, V.

performance, and enhancing squeeze Axial attention with detail enhancement kernel brings a performance boost with a gain of 2.3% mIoU on ADE20K. The results indicate that enhancing global semantic features from squeeze Axial attention with local details from convolution optimizes the feature extraction capability of Transformer block. For enhancement input, there is an apparent performance gap between upconv(x) and conv(x). And we conclude that increasing the channels will boost performance significantly. Comparing concat[qkv] and upconv(x), which also correspond to w/ or w/o convolution weight sharing between detail enhancement kernel and squeeze Axial attention, we can find that sharing weights makes our model improve inference efficiency with minimal performance loss (35.8 vs.35.9). As for enhancement modes, multiplying features from squeeze Axial attention and detail enhancement kernel outperforms add enhancement by +0.4% mIoU.

Comparison with different self-attention modules

In order to eliminate the impact of our architecture and demonstrate the effectiveness and generalization ability of SEA attention, we ran experiments on Swin Transformer Liu et al. (2021) by replacing window attention in Swin Transformer with different attention blocks. We set the same training protocol, hyperparameters, and model architecture configurations as Swin for a fair comparison. When replacing window attention with CCAttention (CCNet) or DoubleAttention (A2-Nets), they have much lower FLOPs than SeaFormer

and other attention blocks. Considering that we may not be able to draw conclusions rigorously, we doubled the number of their Transformer blocks (including MLP). As ACmix has the same architecture configuration as Swin, we borrow the results from the original paper. From Table 4, it can be seen that SeaFormer outperforms other attention mechanisms with lower FLOPs and latency.

Model	Params(B)	FLOPs(B)	mIoU	Latency
Swin	27.5M	25.6G	44.5	3182ms
CCNet	41.6M	37.4G	43.1	3460ms
ISSA	31.8M	33.3G	37.4	2991ms
A2-Nets	37.2M	31.1G	28.9	2502ms
Axial	36.2M	32.5G	45.3	3121ms
Local	27.5M	25.1G	34.2	3059ms
MixFormer	27.5M	24.9G	45.5	2817ms
ACmix	27.9M	26.6G	45.3	3712ms
Global	27.5M	0.144T	OOM	14642ms
SeaFormer	34.0M	24.9G	46.5	2278ms

Table 4: Results on ADE20K *val* set based on Swin Transformer architecture. (B) denotes backbone. OOM means CUDA out of memory. References: ISSA Huang et al. (2019a), A2-Nets Chen et al. (2018b)

The influence of the width in fusion block To study the influence of the width in fusion block, we perform experiments with different embedding dimensions in fusion blocks on SeaFormer-Base, M denotes the channels that spatial branch and context branch features mapping to in two fusion blocks. Results are shown in Table 5.

4.4 IMAGE CLASSIFICATION

We conduct experiments on ImageNet-1K Deng et al. (2009), which contains 1.28M training

images and 50K validation images from 1,000 classes. We employ an AdamW Kingma & Ba (2014) optimizer for 600 epochs using a cosine decay learning rate scheduler. A batch size of 1024, an initial learning rate of 0.064, and a weight decay of $2e-5$ are used. The results are illustrated in Table 6. Compared with other efficient approaches, SeaFormer achieves a relatively better trade-off between latency and accuracy.

M	Params	FLOPs	Latency	mIoU
64,96	8.5M	1.7G	102ms	40.3
128,160	8.6M	1.8G	106ms	41.0
192,256	8.7M	2.0G	121ms	41.2
Posbias	Params	FLOPs	Latency	mIoU
✗	1.65M	0.60G	40ms	35.6
✓	1.67M	0.60G	40ms	35.8

Table 5: Ablation studies on embedding dimensions and position bias. $M = [128, 160]$ is an optimal embedding dimension in fusion blocks.

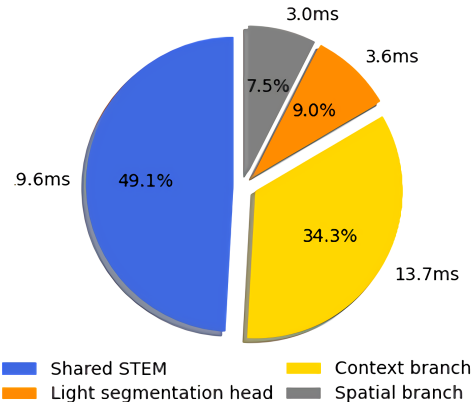


Figure 4: The inference latency of components.

4.5 LATENCY STATISTICS

We make the statistics of the latency of the proposed SeaFormer-Tiny, as shown in Figure 4, the shared STEM takes up about half of the latency of the whole network (49%). The latency of the context branch is about a third of the total latency (34%), whilst the actual latency of the spatial branch is relatively low (8%) due to sharing early convolution layers with the context branch. Our light segmentation head (8%) also contributes to the success of building a light model.

5 CONCLUSION

In this paper, we have proposed *squeeze-enhanced Axial Transformer (SeaFormer)* for mobile semantic segmentation, filling the vacancy of mobile-friendly efficient Transformer. Moreover, we create a family of backbone architectures of SeaFormer and achieve cost-effectiveness. The superior performance on the ADE20K and Cityscapes, and the lowest latency demonstrate its effectiveness on the ARM-based mobile device. Beyond semantic segmentation, we further apply the proposed SeaFormer architecture to image classification problem, demonstrating the potential of serving as a versatile mobile-friendly backbone.

ACKNOWLEDGMENTS

This work was supported in part by National Natural Science Foundation of China (Grant No. 62106050), Lingang Laboratory (Grant No. LG-QS-202202-07), Natural Science Foundation of Shanghai (Grant No. 22ZR1407500) and CCF-Tencent Open Research Fund (No. CCF-Tencent RAGR20210111).

Method	P(M)	F(G)	Top1	L
MobileNetV3-Small	2.9	0.1	67.4	5ms
SeaFormer-T	1.8	0.1	67.9	7ms
MobileViT-XXS	1.3	0.4	69.0	24ms
MobileViTv2-0.50	1.4	0.5	70.2	32ms
MobileOne-S0*	2.1	0.3	71.4	14ms
MobileNetV2	3.4	0.3	72.0	17ms
MobileFormer96	4.8	0.1	72.8	31ms
SeaFormer-S	4.1	0.2	73.3	12ms
EdgeViT-XXS	4.1	0.6	74.4	71ms
LVT	5.5	0.9	74.8	97ms
MobileViT-XS	2.3	0.9	74.8	54ms
MobileNetV3-Large	5.4	0.2	75.2	16ms
MobileFormer151	7.7	0.2	75.2	42ms
MobileViTv2-0.75	2.9	1.0	75.6	68ms
MobileOne-S1*	4.8	0.8	75.9	40ms
SeaFormer-B	8.7	0.3	76.0	20ms
MobileOne-S2*	7.8	1.3	77.4	63ms
EdgeViT-XS	6.8	1.1	77.5	124ms
MobileViTv2-1.00	4.9	1.8	78.1	115ms
MobileOne-S3*	10.1	1.9	78.1	91ms
MobileViT-S	5.6	1.8	78.4	88ms
EfficientNet-B1	7.8	0.7	79.1	61ms
EfficientFormer-L1	12.3	1.3	79.2	94ms
MobileFormer508	14.8	0.5	79.3	102ms
MobileOne-S4*	14.8	3.0	79.4	143ms
SeaFormer-L	14.0	1.2	79.9	61ms

Table 6: Image classification results on ImageNet-1K *val* set. The FLOPs and latency are measured with input size 224×224 , except for MobileViT and MobileViTv2 that are measured with 256×256 according to their original implementations. P, F and L mean Parameters, FLOPs and latency. * indicates re-parameterized variants Vasu et al. (2022). The latency is measured on a single Qualcomm Snapdragon 865, and only an ARM CPU core is used for speed testing. No other means of acceleration, e.g., GPU or quantification, is used.

REFERENCES

- Yue Cao, Jiarui Xu, Stephen Lin, Fangyun Wei, and Han Hu. Gcnet: Non-local networks meet squeeze-excitation networks and beyond. In *ICCV workshops*, 2019.
- Liang-Chieh Chen, George Papandreou, Florian Schroff, and Hartwig Adam. Rethinking atrous convolution for semantic image segmentation. *arXiv preprint*, 2017.
- Liang-Chieh Chen, Yukun Zhu, George Papandreou, Florian Schroff, and Hartwig Adam. Encoder-decoder with atrous separable convolution for semantic image segmentation. In *ECCV*, 2018a.
- Qiang Chen, Qiman Wu, Jian Wang, Qinghao Hu, Tao Hu, Errui Ding, Jian Cheng, and Jingdong Wang. Mixformer: Mixing features across windows and dimensions. In *CVPR*, 2022a.
- Yinpeng Chen, Xiyang Dai, Dongdong Chen, Mengchen Liu, Xiaoyi Dong, Lu Yuan, and Zicheng Liu. Mobile-former: Bridging mobilenet and transformer. In *CVPR*, 2022b.
- Yunpeng Chen, Yannis Kalantidis, Jianshu Li, Shuicheng Yan, and Jiashi Feng. A²-nets: Double attention networks. In *NeurIPS*, 2018b.
- Krzysztof Choromanski, Valerii Likhoshesterov, David Dohan, Xingyou Song, Andreea Gane, Tamas Sarlos, Peter Hawkins, Jared Davis, Afroz Mohiuddin, Lukasz Kaiser, et al. Rethinking attention with performers. In *ICLR*, 2021.
- MMSegmentation Contributors. Mmsegmentation: Openmmlab semantic segmentation toolbox and benchmark, 2020.
- TNN Contributors. Tnn: A high-performance, lightweight neural network inference framework., 2019.
- Marius Cordts, Mohamed Omran, Sebastian Ramos, Timo Rehfeld, Markus Enzweiler, Rodrigo Benenson, Uwe Franke, Stefan Roth, and Bernt Schiele. The cityscapes dataset for semantic urban scene understanding. In *CVPR*, 2016.
- Jia Deng, Wei Dong, Richard Socher, Li-Jia Li, Kai Li, and Li Fei-Fei. Imagenet: A large-scale hierarchical image database. In *CVPR*, 2009.
- Alexey Dosovitskiy, Lucas Beyer, Alexander Kolesnikov, Dirk Weissenborn, Xiaohua Zhai, Thomas Unterthiner, Mostafa Dehghani, Matthias Minderer, Georg Heigold, Sylvain Gelly, et al. An image is worth 16x16 words: Transformers for image recognition at scale. In *ICLR*, 2021.
- Hongyang Gao, Zhengyang Wang, and Shuiwang Ji. Kronecker attention networks. In *ACM SIGKDD*, 2020.
- Kaiming He, Xiangyu Zhang, Shaoqing Ren, and Jian Sun. Deep residual learning for image recognition. In *CVPR*, 2016.
- Jonathan Ho, Nal Kalchbrenner, Dirk Weissenborn, and Tim Salimans. Axial attention in multidimensional transformers. *arXiv preprint*, 2019.
- Yuanduo Hong, Huihui Pan, Weichao Sun, and Yisong Jia. Deep dual-resolution networks for real-time and accurate semantic segmentation of road scenes. *arXiv preprint*, 2021.
- Qibin Hou, Li Zhang, Ming-Ming Cheng, and Jiashi Feng. Strip pooling: Rethinking spatial pooling for scene parsing. In *CVPR*, 2020.
- Qibin Hou, Daquan Zhou, and Jiashi Feng. Coordinate attention for efficient mobile network design. In *CVPR*, 2021.
- Andrew Howard, Mark Sandler, Grace Chu, Liang-Chieh Chen, Bo Chen, Mingxing Tan, Weijun Wang, Yukun Zhu, Ruoming Pang, Vijay Vasudevan, et al. Searching for mobilenetv3. In *ICCV*, 2019.
- Lang Huang, Yuhui Yuan, Jianyuan Guo, Chao Zhang, Xilin Chen, and Jingdong Wang. Interlaced sparse self-attention for semantic segmentation. *arXiv preprint*, 2019a.
- Zilong Huang, Xinggang Wang, Lichao Huang, Chang Huang, Yunchao Wei, and Wenyu Liu. Ccnet: Criss-cross attention for semantic segmentation. In *ICCV*, 2019b.
- Zilong Huang, Youcheng Ben, Guozhong Luo, Pei Cheng, Gang Yu, and Bin Fu. Shuffle transformer: Rethinking spatial shuffle for vision transformer. *arXiv preprint*, 2021a.

- Zilong Huang, Yunchao Wei, Xinggang Wang, Wenyu Liu, Thomas S Huang, and Humphrey Shi. Alignseg: Feature-aligned segmentation networks. *TPAMI*, 2021b.
- Sergey Ioffe and Christian Szegedy. Batch normalization: Accelerating deep network training by reducing internal covariate shift. In *ICML*, 2015.
- Diederik P Kingma and Jimmy Ba. Adam: A method for stochastic optimization. *arXiv preprint*, 2014.
- Alexander Kirillov, Ross Girshick, Kaiming He, and Piotr Dollár. Panoptic feature pyramid networks. In *CVPR*, 2019.
- Hanchao Li, Pengfei Xiong, Haoqiang Fan, and Jian Sun. Dfanet: Deep feature aggregation for real-time semantic segmentation. In *CVPR*, 2019.
- Jiachen Li, Ali Hassani, Steven Walton, and Humphrey Shi. Convmlp: Hierarchical convolutional mlps for vision. *arXiv preprint*, 2021a.
- Xiangtai Li, Xia Li, Li Zhang, Guangliang Cheng, Jianping Shi, Zhouchen Lin, Shaohua Tan, and Yunhai Tong. Improving semantic segmentation via decoupled body and edge supervision. In *ECCV*, 2020.
- Xiangtai Li, Xia Li, Ansheng You, Li Zhang, Guangliang Cheng, Kuiyuan Yang, Yunhai Tong, and Zhouchen Lin. Towards efficient scene understanding via squeeze reasoning. *TIP*, 2021b.
- Xiangtai Li, Li Zhang, Guangliang Cheng, Kuiyuan Yang, Yunhai Tong, Xiatian Zhu, and Tao Xiang. Global aggregation then local distribution for scene parsing. *TIP*, 2021c.
- Yanyu Li, Geng Yuan, Yang Wen, Eric Hu, Georgios Evangelidis, Sergey Tulyakov, Yanzhi Wang, and Jian Ren. Efficientformer: Vision transformers at mobilenet speed. *arXiv preprint*, 2022.
- Tsung-Yi Lin, Priya Goyal, Ross Girshick, Kaiming He, and Piotr Dollár. Focal loss for dense object detection. In *ICCV*, 2017.
- Peter J Liu, Mohammad Saleh, Etienne Pot, Ben Goodrich, Ryan Sepassi, Lukasz Kaiser, and Noam Shazeer. Generating wikipedia by summarizing long sequences. In *ICLR*, 2018.
- Ze Liu, Yutong Lin, Yue Cao, Han Hu, Yixuan Wei, Zheng Zhang, Stephen Lin, and Baining Guo. Swin transformer: Hierarchical vision transformer using shifted windows. In *ICCV*, 2021.
- Jonathan Long, Evan Shelhamer, and Trevor Darrell. Fully convolutional networks for semantic segmentation. In *CVPR*, 2015.
- Minh-Thang Luong, Hieu Pham, and Christopher D Manning. Effective approaches to attention-based neural machine translation. *arXiv preprint*, 2015.
- Ningning Ma, Xiangyu Zhang, Hai-Tao Zheng, and Jian Sun. Shufflenet v2: Practical guidelines for efficient cnn architecture design. In *ECCV*, 2018.
- Sachin Mehta and Mohammad Rastegari. Mobilevit: light-weight, general-purpose, and mobile-friendly vision transformer. In *ICLR*, 2022a.
- Sachin Mehta and Mohammad Rastegari. Separable self-attention for mobile vision transformers. *arXiv preprint*, 2022b.
- Junting Pan, Adrian Bulat, Fuwen Tan, Xiatian Zhu, Lukasz Dudziak, Hongsheng Li, Georgios Tzimiropoulos, and Brais Martinez. Edgevits: Competing light-weight cnns on mobile devices with vision transformers. In *ECCV*, 2022a.
- Xuran Pan, Chunjiang Ge, Rui Lu, Shiji Song, Guanfu Chen, Zeyi Huang, and Gao Huang. On the integration of self-attention and convolution. In *CVPR*, 2022b.
- Rudra PK Poudel, Stephan Liwicki, and Roberto Cipolla. Fast-scnn: Fast semantic segmentation network. In *BMVC*, 2019.
- Mark Sandler, Andrew Howard, Menglong Zhu, Andrey Zhmoginov, and Liang-Chieh Chen. Mobilenetv2: Inverted residuals and linear bottlenecks. In *CVPR*, 2018.
- Zhuoran Shen, Mingyuan Zhang, Haiyu Zhao, Shuai Yi, and Hongsheng Li. Efficient attention: Attention with linear complexities. In *WACV*, 2021.

- Mingxing Tan and Quoc Le. Efficientnet: Rethinking model scaling for convolutional neural networks. In *ICML*, 2019.
- Pavan Kumar Anasosalu Vasu, James Gabriel, Jeff Zhu, Oncel Tuzel, and Anurag Ranjan. An improved one millisecond mobile backbone. *arXiv preprint*, 2022.
- Ashish Vaswani, Noam Shazeer, Niki Parmar, Jakob Uszkoreit, Llion Jones, Aidan N Gomez, Łukasz Kaiser, and Illia Polosukhin. Attention is all you need. In *NeurIPS*, 2017.
- Huiyu Wang, Yukun Zhu, Bradley Green, Hartwig Adam, Alan Yuille, and Liang-Chieh Chen. Axial-deeplab: Stand-alone axial-attention for panoptic segmentation. In *ECCV*, 2020a.
- Sinong Wang, Belinda Z Li, Madian Khabsa, Han Fang, and Hao Ma. Linformer: Self-attention with linear complexity. *arXiv preprint*, 2020b.
- Wenhai Wang, Enze Xie, Xiang Li, Deng-Ping Fan, Kaitao Song, Ding Liang, Tong Lu, Ping Luo, and Ling Shao. Pyramid vision transformer: A versatile backbone for dense prediction without convolutions. In *ICCV*, 2021.
- Sanghyun Woo, Jongchan Park, Joon-Young Lee, and In So Kweon. Cbam: Convolutional block attention module. In *ECCV*, 2018.
- Enze Xie, Wenhai Wang, Zhiding Yu, Anima Anandkumar, Jose M Alvarez, and Ping Luo. Segformer: Simple and efficient design for semantic segmentation with transformers. In *NeurIPS*, 2021.
- Weijian Xu, Yifan Xu, Tyler Chang, and Zhuowen Tu. Co-scale conv-attentional image transformers. In *ICCV*, 2021.
- Haotian Yan, Zhe Li, Weijian Li, Changhu Wang, Ming Wu, and Chuang Zhang. Contnet: Why not use convolution and transformer at the same time? *arXiv preprint*, 2021.
- Chenglin Yang, Yilin Wang, Jianming Zhang, He Zhang, Zijun Wei, Zhe Lin, and Alan Yuille. Lite vision transformer with enhanced self-attention. In *CVPR*, 2022.
- Changqian Yu, Jingbo Wang, Chao Peng, Changxin Gao, Gang Yu, and Nong Sang. Bisenet: Bilateral segmentation network for real-time semantic segmentation. In *ECCV*, 2018.
- Changqian Yu, Changxin Gao, Jingbo Wang, Gang Yu, Chunhua Shen, and Nong Sang. Bisenet v2: Bilateral network with guided aggregation for real-time semantic segmentation. *IJCV*, 2021.
- Yuhui Yuan, Xilin Chen, and Jingdong Wang. Object-contextual representations for semantic segmentation. In *ECCV*, 2020.
- Yuhui Yuan, Rao Fu, Lang Huang, Weihong Lin, Chao Zhang, Xilin Chen, and Jingdong Wang. Hrformer: High-resolution transformer for dense prediction. *arXiv preprint*, 2021.
- Haokui Zhang, Wenze Hu, and Xiaoyu Wang. Edgeformer: Improving light-weight convnets by learning from vision transformers. *arXiv preprint*, 2022a.
- Li Zhang, Dan Xu, Anurag Arnab, and Philip HS Torr. Dynamic graph message passing networks. In *CVPR*, 2020.
- Li Zhang, Mohan Chen, Anurag Arnab, Xiangyang Xue, and Philip HS Torr. Dynamic graph message passing networks for visual recognition. *TPAMI*, 2022b.
- Wenqiang Zhang, Zilong Huang, Guozhong Luo, Tao Chen, Xinggong Wang, Wenyu Liu, Gang Yu, and Chunhua Shen. Topformer: Token pyramid transformer for mobile semantic segmentation. In *CVPR*, 2022c.
- Hengshuang Zhao, Xiaojuan Qi, Xiaoyong Shen, Jianping Shi, and Jiaya Jia. Icnet for real-time semantic segmentation on high-resolution images. In *ECCV*, 2018.
- Sixiao Zheng, Jiachen Lu, Hengshuang Zhao, Xiatian Zhu, Zekun Luo, Yabiao Wang, Yanwei Fu, Jianfeng Feng, Tao Xiang, Philip HS Torr, et al. Rethinking semantic segmentation from a sequence-to-sequence perspective with transformers. In *CVPR*, 2021.
- Bolei Zhou, Hang Zhao, Xavier Puig, Sanja Fidler, Adela Barriuso, and Antonio Torralba. Scene parsing through ade20k dataset. In *CVPR*, 2017.

Appendix

A ARCHITECTURE DETAILS AND VARIANTS

SeaFormer backbone contains 6 stages, corresponding to the shared STEM and context branch in Figure 2 in the main paper. When conducting the image classification experiments, a pooling layer and a linear layer are added at the end of the context branch.

Table 7 details the family of our SeaFormer configurations with varying capacities. We construct SeaFormer-Tiny, SeaFormer-Small, SeaFormer-Base and SeaFormer-Large models with different scales via varying the number of SeaFormer layers and the feature dimensions. We use input image size of 512×512 by default. For variants except SeaFormer-Large, SeaFormer layers are applied in the last two stages for superior trade-off between accuracy and efficiency. For SeaFormer-Large, we apply the proposed SeaFormer layers in each stage of the context branch.

B COMPLEXITY ANALYSIS

we analyze the complexity of our proposed SEA attention in subsection 3.2 to demonstrate its efficiency theoretically. In our application, we set $C_{qk} = 0.5C_v$ to further reduce computation cost. The total time complexity of squeeze-enhanced Axial attention is

$$\begin{aligned} & \mathcal{O}((H^2 + W^2)(C_{qk} + C_v) + \mathcal{O}((H + W)(2C_{qk} + C_v)) + \mathcal{O}((HWC + 9HW)(2C_{qk} + C_v)) \\ & = \mathcal{O}((1.5H^2 + 1.5W^2 + 2HWC + 18HW + 2H + 2W)C_v) = \mathcal{O}(HW), \end{aligned} \quad (7)$$

if we assume $H = W$ and take channel as constant. SEA attention is linear to the feature map size theoretically. Moreover, SEA attention only includes mobile-friendly operation like convolution, pooling, matrix multiplication and so on.

C PASCAL CONTEXT PERFORMANCE

We evaluate performance on Pascal Context *val* set over 59 categories and 60 categories. **PASCAL Context** dataset has 4998/5105 images for *train* and *test*, covering 59 semantic labels and 1 background.

Following TopFormer Zhang et al. (2022c), we train the models for 80,000 iterations on PASCAL Context dataset. The same data augmentation strategy and batch size are adopted for a fair comparison. The initial learning rate is 0.0002 and the weight decay is 0.01. A poly learning rate scheduled with factor 1.0 is used.

Table 8 demonstrates that SeaFormer-S is +1.4% mIoU higher (45.08% vs.43.68%) than TopFormer-S with lower latency.

D COCO-STUFF PERFORMANCE

We compare SeaFormer with the previous approaches on COCO-Stuff *val* set. **COCO-Stuff** dataset augments COCO dataset with pixel-level stuff annotations. 10K complex images are selected from COCO. The *train* and *test* set contain 9K/1K images.

Following TopFormer Zhang et al. (2022c), we train the models for 80,000 iterations on COCO-Stuff dataset. The same data augmentation strategy and batch size are adopted for a fair comparison. The initial learning rate is 0.0002 and the weight decay is 0.01. A poly learning rate scheduled with factor 1.0 is used.

Table 9 reveals that SeaFormer-S is +2.0% mIoU higher (32.82% vs.30.83%) than TopFormer-S with less computation cost and lower latency.

	Resolution	SeaFormer-Tiny	SeaFormer-Small	SeaFormer-Base	SeaFormer-Large
Stage1	H/2 × W/2	[Conv, 3, 16, 2] [MB, 3, 1, 16, 1]	[Conv, 3, 16, 2] [MB, 3, 1, 16, 1]	[Conv, 3, 16, 2] [MB, 3, 1, 16, 1]	[Conv, 3, 32, 2] [MB, 3, 3, 32, 1]
Stage2	H/4 × W/4	[MB, 3, 4, 16, 2] [MB, 3, 3, 16, 1]	[MB, 3, 4, 24, 2] [MB, 3, 3, 24, 1]	[MB, 3, 4, 32, 2] [MB, 3, 3, 32, 1]	[MB, 3, 4, 64, 2] [MB, 3, 4, 64, 1]
Stage3	H/8 × W/8	[MB, 5, 3, 32, 2] [MB, 5, 3, 32, 1]	[MB, 5, 3, 48, 2] [MB, 5, 3, 48, 1]	[MB, 5, 3, 64, 2] [MB, 5, 3, 64, 1]	[MB, 5, 4, 128, 2] [MB, 5, 4, 128, 1]
Stage4	H/16 × W/16	[MB, 3, 3, 64, 2] [MB, 3, 3, 64, 1]	[MB, 3, 3, 96, 2] [MB, 3, 3, 96, 1]	[MB, 3, 3, 128, 2] [MB, 3, 3, 128, 1]	[MB, 3, 4, 192, 2] [MB, 3, 4, 192, 1] [Sea, 3, 8]
Stage5	H/32 × W/32	[MB, 5, 3, 128, 2] [Sea, 2, 4]	[MB, 5, 4, 160, 2] [Sea, 3, 6]	[MB, 5, 4, 192, 2] [Sea, 4, 8]	[MB, 5, 4, 256, 2] [Sea, 3, 8]
Stage6	H/64 × W/64	[MB, 3, 6, 160, 2] [Sea, 2, 4]	[MB, 3, 6, 192, 2] [Sea, 3, 6]	[MB, 3, 6, 256, 2] [Sea, 4, 8]	[MB, 3, 6, 320, 2] [Sea, 3, 8]

Table 7: Architectures for semantic segmentation. [Conv, 3, 16, 2] denotes regular convolution layer with kernel of 3, output channel of 16 and stride of 2. [MB, 3, 4, 16, 2] means MobileNetV2 Sandler et al. (2018) block with kernel of 3, expansion ratio of 4, output channel of 16 and stride of 2. [Sea, 2, 4] refers to SeaFormer layers with number of layers of 2 and heads of 4.

Backbone	Decoder	F(G)	mIoU(60/59)
MBV2-s16	DeepLabV3+	22.24	38.59/42.34
ENet-s16	DeepLabV3+	23.00	39.19/43.07
MBV3-s16	LR-ASPP	2.04	35.05/38.02
TopFormer-T	Simple Head	0.53	36.41/40.39
SeaFormer-T	Light Head	0.51	37.27/41.49
TopFormer-S	Simple Head	0.98	39.06/43.68
SeaFormer-S	Light Head	0.98	40.20/45.08
TopFormer-B	Simple Head	1.54	41.01/45.28
SeaFormer-B	Light Head	1.57	41.77/45.92

Table 8: Results on Pascal Context *val* set. F means FLOPs. We omit the latency as the input resolution is almost the same as that in table 1.

Backbone	Decoder	F(G)	mIoU
MBV2-s8	PSPNet	52.94	30.14
ENet-s16	DeepLabV3+	27.10	31.45
MBV3-s16	LR-ASPP	2.37	25.16
TopFormer-T	Simple Head	0.64	28.34
SeaFormer-T	Light Head	0.62	29.24
TopFormer-S	Simple Head	1.18	30.83
SeaFormer-S	Light Head	1.15	32.82
TopFormer-B	Simple Head	1.83	33.43
SeaFormer-B	Light Head	1.81	34.07

Table 9: Results on COCO-Stuff *test* set. F means FLOPs. We omit the latency in this table as the input resolution is the same as that in table 1.

Backbone	AP	FLOPs	Params
ShuffleNetv2 Ma et al. (2018)	25.9	161G	10.4M
SeaFormer-T	31.5	160G	10.9M
MF151	34.2	161G	14.4M
MV3	27.2	162G	12.3M
SeaFormer-S	34.6	161G	13.3M
MF214	35.8	162G	15.2M
MF294	36.6	164G	16.1M
SeaFormer-B	36.7	164G	18.1M
ResNet50 He et al. (2016)	36.5	239G	37.7M
PVT-Tiny Wang et al. (2021)	36.7	221G	23.0M
ConT-M Yan et al. (2021)	37.9	217G	27.0M
SeaFormer-L	39.8	185G	24.0M

Table 10: Results on COCO object detection. MF denotes Mobile-Former Chen et al. (2022b). MV3 denotes MobileNetV3 Howard et al. (2019).

Fusion method	mIoU
Add directly	35.2
Multiply directly	35.2
Sigmoid add	34.8
Sigmoid multiply	35.8

Table 11: Ablation study on fusion method on ADE20K *val* set.

E OBJECT DETECTION PERFORMANCE

To further demonstrate the generalization ability of our proposed SeaFormer backbone on other downstream tasks, we conduct object detection task on COCO dataset.

Setup We use RetinaNet Lin et al. (2017) (one-stage) as the detection framework and follow the standard settings to use SeaFormer as backbone to generate a feature pyramid at multiple scales. All models are trained on train2017 split for 12 epochs (1×) from ImageNet pretrained weights.

Results From the table 10 We can observe that our SeaFormer achieves superior results on detection task which further demonstrates the strong generalization ability of our method.

F ADDITIONAL ABLATION STUDY

In addition to the ablation study in the submission paper, we investigate the effect of fusion method in fusion block in Figure 2.

F.1 THE INFLUENCE OF FUSION BLOCK DESIGN

We set four fusion methods, including "Add directly", "Multiply directly", "Sigmoid add" and "Sigmoid multiply". \mathbf{X} directly means features from context branch and spatial branch \mathbf{X} directly. Sigmoid \mathbf{X} means feature from context branch goes through a sigmoid layer and \mathbf{X} feature from spatial branch.

From the Table 11 we can see that replacing sigmoid multiply with other fusion methods hurts performance. Sigmoid multiply is our optimal fusion block choice.

F.2 EFFECTIVE AND EFFICIENCY OF SEA ATTENTION

To verify the effectiveness and efficiency of SEA attention based on our designed pipeline, we experiment with convolution, Global attention, Local attention, Axial attention and three convolution

Method	Params	FLOPs	Latency	Top1	mIoU
Conv	1.6M	0.59G	38ms	66.3	32.8
Local	1.3M	0.60G	48ms	65.9	32.8
Axial	1.6M	0.63G	44ms	66.9	33.7
Global	1.3M	0.61G	43ms	66.7	34.2
ACmix	1.3M	0.60G	54ms	66.0	33.1
MixFormer	1.3M	0.60G	50ms	66.8	33.8
SeaFormer	1.7M	0.60G	40ms	67.9	35.8

Table 12: Performance of different self-attention modules on our designed pipeline on ImageNet-1K and ADE20K datasets.

Model	mIoU	FP32	FP16
TopFormer-T	34.6	43ms	23ms
SeaFormer-T	35.8	40ms	22ms
TopFormer-S	37.0	74ms	41ms
SeaFormer-S	39.4	67ms	36ms
TopFormer-B	39.2	110ms	60ms
SeaFormer-B	41.0	106ms	56ms
SeaFormer-L	43.7	367ms	186ms

Table 13: Performance comparison on ADE20K *val* set under different precision.

enhanced attention methods including our SEA attention, ACmix and MixFormer. The ablation experiments are organized in seven groups. Since the resolution of computing attention is relatively small, the window size in Local attention, ACmix, and MixFormer is set to 4. We adjust the channels when applying different attention modules to keep the FLOPs aligned and compare their performance and latency. The results are illustrated in Table 12.

As demonstrated in the table, SEA attention outperforms the counterpart built on other efficient attentions. Compared with global attention, SEA attention outperforms it by +1.2% Top1 accuracy on ImageNet-1K and +1.6 mIoU on ADE20K with less FLOPs and lower latency. Compared with similar convolution enhanced attention works, ACmix and MixFormer, our SEA attention obtains better results on ImageNet-1K and ADE20K with similar FLOPs but lower latency. The results indicate the effectiveness and efficiency of SEA attention module.

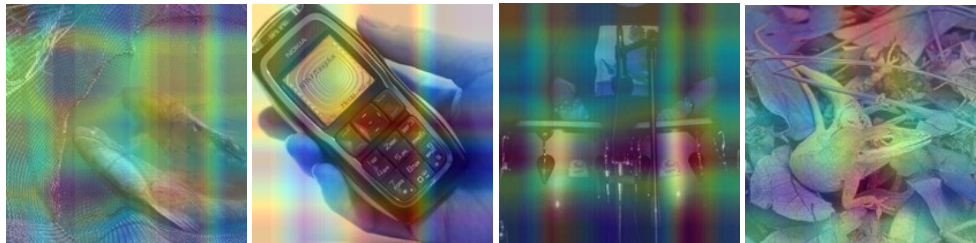
G PERFORMANCE UNDER DIFFERENT PRECISION OF THE MODELS

Following TopFormer, we measure the latency in the submission paper on a single Qualcomm Snapdragon 865, and only an ARM CPU core is used for speed testing. No other means of acceleration, e.g., GPU or quantification, is used. We provide a more comprehensive comparison to demonstrate the necessity of our proposed method. We test the latency under different precision of the models. From the table 13, it can be seen that whether it is full precision or half precision the performance of SeaFormer is better than that of TopFormer.

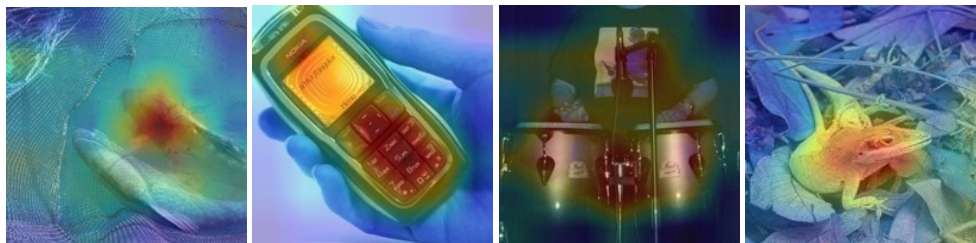
H VISUALIZATION

H.1 ATTENTION HEATMAP

To demonstrate the effectiveness of detail enhancement in our squeeze-enhanced Axial attention (SEA attention), we ablate our model by removing the detail enhancement. We visualize the attention heatmaps of the two models in Figure 5. Without detail enhancement, attention heatmaps from solely SA attention appears to be axial strips while our proposed SEA attention is able to activate the semantic local region accurately, which is particularly significant in the dense prediction task.



(a) Squeeze Axial attention heatmaps



(b) Squeeze-enhanced Axial attention heatmaps

Figure 5: The visualization of attention heatmaps from the model consisting of squeeze Axial attention without detail enhancement (*first row*) and SeaFormer (*second row*). Heatmaps are produced by averaging channels of the features from the last attention block, normalizing to $[0, 255]$ and up-sampling to the image size.

H.2 PREDICTION RESULTS

We show the qualitative results and compare with the alternatives on the ADE20K validation set from two different perspectives. First we compare with a mobile-friendly rival TopFormer Zhang et al. (2022c) with similar FLOPs and latency in Figure 6. Besides, we compare with the Transformer-based counterpart SegFormer-B1 Xie et al. (2021) in Figure 7. In particular, our SeaFormer-L has lower computation cost than the SegFormer-B1. As shown in both figures, we demonstrate better segmentation results than both the mobile counterpart and Transformer-based approach.

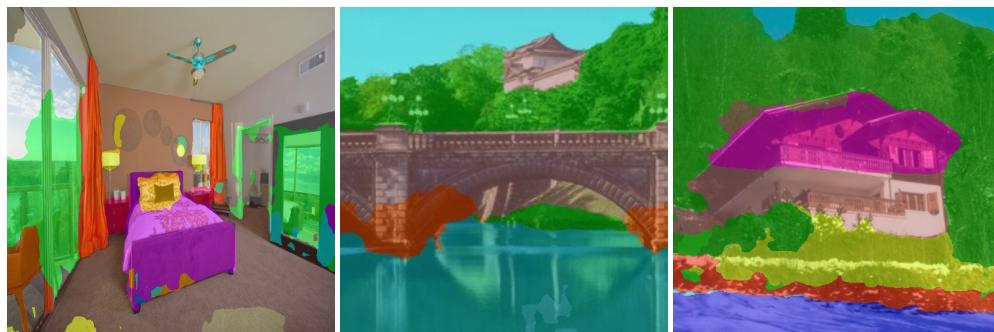
I LIMITATIONS AND SOCIETAL IMPACT

The mobile-friendly segmentation is deeply related to the industrial application on edge computation platforms, while few academic attempts are made to meet the requirement of the industry. We test our method on a Qualcomm Snapdragon 865 processor (Fig.1 main paper) and shows superior results to the alternatives. We believe our work can lead to expected and unexpected innovations in both academia and industry.

However, our system is not perfect yet and hence not fully trustworthy in real-world deployment. Also, the current system is not exhaustively evaluated and tested due to limited resources. We focus on mobile semantic segmentation and image classification tasks. New mobile-friendly method for more downstream tasks and extended to GPU systems will be studied in the future.



(a) Ground Truth



(b) TopFormer-B Zhang et al. (2022c)

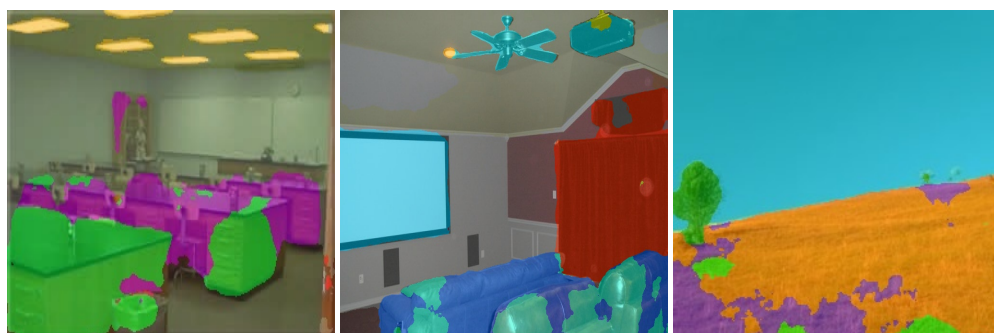


(c) SeaFormer-B (Ours)

Figure 6: Visualization of prediction results on ADE20K *val* set.



(a) Ground Truth



(b) SegFormer-B1 Xie et al. (2021)



(c) SeaFormer-L (Ours)

Figure 7: Visualization of prediction results on ADE20K *val* set.